Temporal variations of CO infrared lines in cool star winds

A. Gauger[1], J.M. Winters[2], A.J. Fleischer[2], and J.J. Keady[3]

[1] Max–Planck–Institut für Radioastronomie,
Auf dem Hügel 69, 53121 Bonn, FRG

[2] Institut für Astronomie und Astrophysik, TU Berlin,
PN8-1, Hardenbergstr. 36, 10623 Berlin, FRG

[3] Los Alamos National Laboratory, Theoretical Division,
Group T–4, MS B212, Los Alamos, NM 87545, USA

1 Introduction

Almost all Miras and most long–period variables (LPVs) are highly evolved low and intermediate mass stars located on the Asymptotic Giant Branch (AGB). These objects are large amplitude pulsators with typical periods of the order of 1 yr, high luminosities $\approx 10^4 \mathrm{L}_\odot$, and low effective temperatures < 3000K. In this evolutionary state, the stars develop a **slow cool massive dusty wind** with typical velocities of $10 - 20$ kms^{-1}, resulting in mass loss rates up to 10^{-4} $\mathrm{M}_\odot \mathrm{yr}^{-1}$ (Habing 1990).

The development and the properties of these winds are commonly believed to be the result of a two–step mechanism:

1. levitation of the atmosphere due to the cyclical passage of shock waves generated by the interior pulsation, and
2. acceleration of the matter by radiation pressure on dust grains, which condense in the region with sufficient density enhancement.

Since dust formation depends sensitively on the local conditions, which in turn are substantially affected by the presence of dust, there results a complex interaction between the dust component and the time–dependent structure of the wind (Fleischer et al. 1992, 1995), which manifests itself in the derived observable properties (Winters et al. 1994, 1995).

To study the structure and dynamics of cool star winds the CO molecule is an especially well suited diagnostic probe, because it is one of the most abundant species in both, oxygen–rich and in carbon–rich objects. Due to its stability CO already forms at high temperatures deep in the photosphere and remains chemically inert out to large distances. For example, values for the terminal velocity of the wind are derived quite accurately from microwave emission lines of CO rotational transitions in the vibrational ground state (Knapp 1987), and direct evidence for the passage of shocks through the photosphere has been provided by Hinkle et al. (1984) from the analysis of time series spectra of the CO $\Delta v = 3$ infrared lines.

In this contribution we present the results of non–LTE radiative transfer calculations for CO infrared lines, which are based on the structure of dynamical dust shell models. The resulting synthetic line profiles and their time evolution are discussed in terms of the wind structure and compared to high resolution CO line spectra obtained for the carbon–rich Mira IRC+10216.

2 Observations of CO infrared lines of IRC+10216

CO infrared absorption lines emerge from the inner parts of the wind, where the flow starts and accelerates. Therefore high resolution IR spectroscopy, which resolves individual vibration rotation lines, can reveal considerable details about the dynamics in this region (Keady et al. 1988).

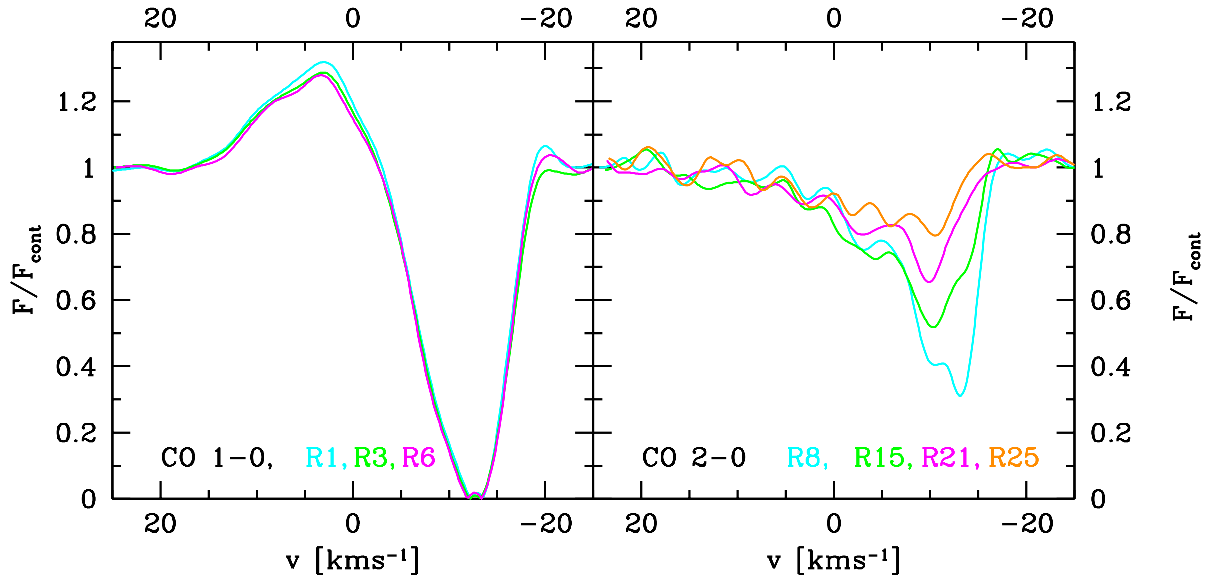

Figure 1: Observed CO infrared line spectra of IRC+10216 obtained on Nov 6, 1981: a) CO fundamental $v = 1 - 0$ transitions, b) CO first overtone $v = 2 - 0$ transitions. Blueshifted lines are at negative velocities.

Figure 1 shows observed CO line spectra of $v = 1 - 0$ fundamental band lines ($\lambda \approx 5\,\mu$m) and $v = 2 - 0$ first overtone band lines ($\lambda \approx 2\,\mu$m). The fundamental band lines show the classic P Cygni profiles with an emission component of $\approx 25\%$ above the continuum and an extremely saturated blueshifted absorption core at $\approx -14\,\mathrm{kms}^{-1}$. Owing to the saturation the most useful information is provided by the P Cygni emission component, which constrains the dust optical depth at $5\,\mu$m to values between about $2 - 4$, because otherwise either too much or too little emission will result. In contrast the first overtone transitions are much less saturated due to their decreased oscillator strength, and little P Cygni emission is expected because after an excitation from $v = 0$ to $v = 2$ subsequent decay to $v = 1$ is more likely than to the $v = 0$ state. The lines show a multicomponent absorption structure extending out to $-14\,\mathrm{kms}^{-1}$, and the location and strength of the individual absorption components (e.g. at $-10\,\mathrm{kms}^{-1}$) depends on the rotational excitation. This makes them suitable to probe the velocity field in the acceleration region of the wind, because lines of increasing excitation presumably form at decreasing distance from the star.

3 Dynamical models of circumstellar dust shells around long–period variables

3.1 The modeling method

Our approach to model circmstellar dust shells around Miras and LPVs is described in detail in Fleischer et al. (1992). It comprises

- the explicit solution of the time dependent hydro–equations in Lagrangian coordinates for a spherical symmetric geometry according to the scheme of Richtmyer & Morton (1967),
- a detailed treatment of the formation, growth and evaporation of carbon grains by means of the moment method (Gail & Sedlmayr 1988, Gauger et al. 1990), which includes an equilibrium chemistry for the important hydrocarbons,
- an approximate treatment of radiative transfer in terms of frequency integrated moments by a generalized Eddington approximation for a spherical, gray atmosphere (Lucy 1976, Hashimoto 1995),
- the description of postshock cooling of the gas either by limiting cases (e.g. isothermal shocks) or by parameterized cooling functions (cf. Bowen 1988),
- the simulation of the interior pulsation by a sinusodially moving inner boundary (piston).

The models are determined by the four stellar parameters mass M_*, luminosity L_*, effective temperature T_*, and abundances of elements ϵ_i (especially the carbon abundance ϵ_C), and by the period P and velocity amplitude Δv_P of the piston.

The values adopted for the present dust shell model of IRC+10216 are:

$$\begin{aligned}
M_* &= 0.8\,\mathrm{M}_\odot \\
L_* &= 8000\,\mathrm{L}_\odot \\
T_* &= 3000\,\mathrm{K} \\
\epsilon_\mathrm{C} &= 1.3\,\epsilon_\mathrm{O} \\
P &= 650\,\mathrm{d} \\
\Delta v_P &= 8.0\,\mathrm{km\,s^{-1}}
\end{aligned}$$

3.2 Structure of the dust shell model

The resulting values of the mass loss rate, the final outflow velocity, and the dust–to–gas ratio for the calculated dust shell model are :

$$\begin{aligned} \dot{M} &= 3.5\ 10^{-5}\ \mathrm{M}_\odot\,\mathrm{yr}^{-1} \\ v_\infty &= 13.5\ \mathrm{km\,s}^{-1} \\ \rho_d/\rho_g &= 1.2\ 10^{-3} \end{aligned}$$

Figure 2 shows the radial structure of our dynamical dust shell model for IRC+10216 at the same phase in two successive pulsational cycles.

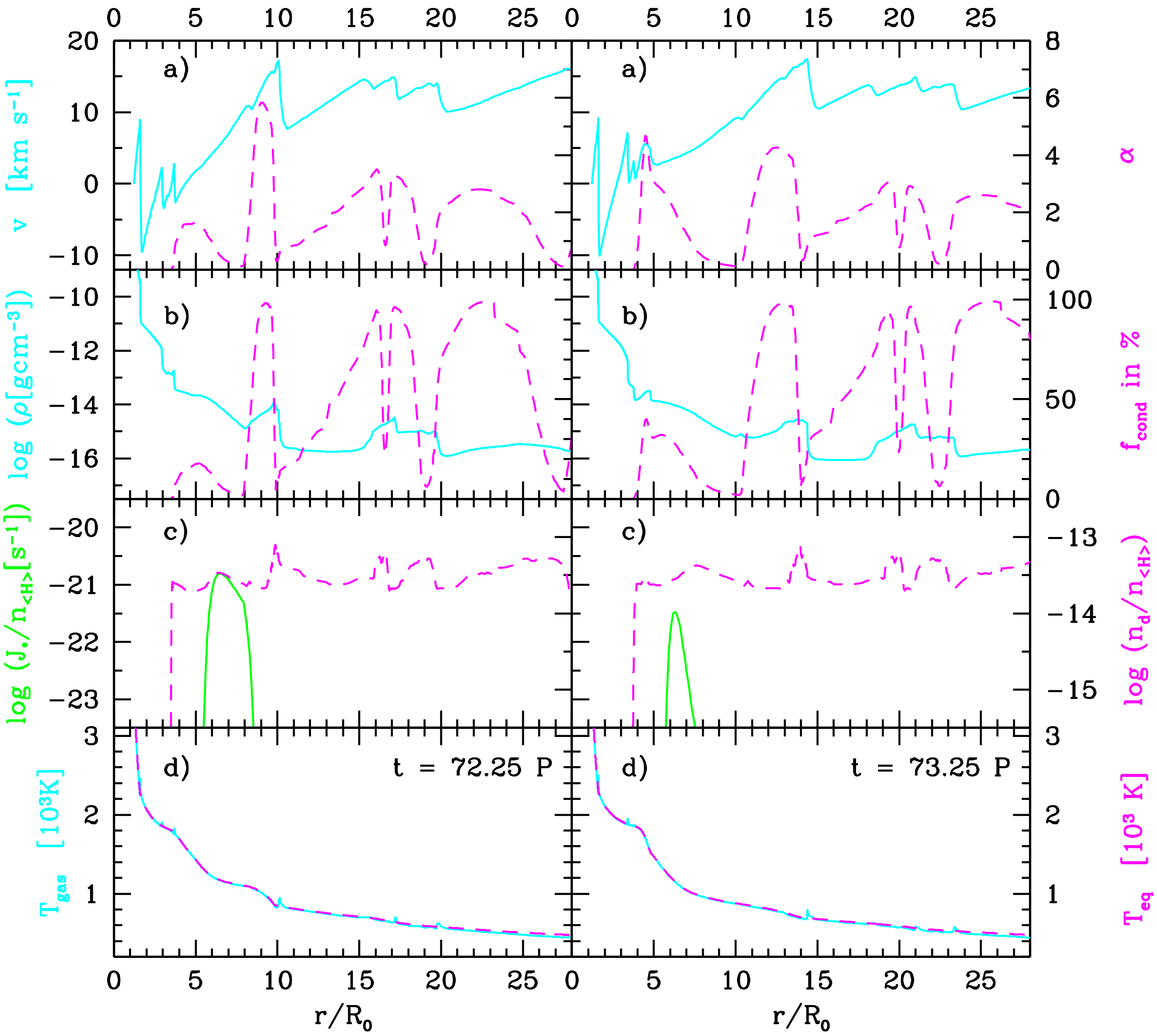

Figure 2: Radial structure of the dust shell model at t = 72.25 P and t = 73.25 P
a) velocity v and radiative acceleration on dust α,
b) density ρ and degree of condensation f_{cond}, i.e. fraction of C–atoms not bound in CO, which are condensed into grains,
c) grain formation rate $J_*/n_{<H>}$, i.e. number of grains formed per second and H–atom, and number of grains per H–atom $n_d/n_{<H>}$,
d) gas temperature T_{gas} and radiative equilibrium temperature T_{eq}.

The dust formation process depends sensitively on the local temperature and density, which vary substantially in the inner parts of the atmosphere, due to the passage of shocks generated by the interior pulsation. Therefore grains can form only in a limited radius intervall and during certain phases of the cycle. On the other hand, radiation pressure on dust substantially affects the hydro– and thermodynamical structure of the flow. This interaction leads to a variety of **dust induced dynamical phenomena** (Fleischer et al. 1991, 1992):

1. Strong shocks dominating the shell structure, which are either generated by pulsation and amplified by radiation pressure on newly formed grains, or even produced by the radiation pressure alone (Fig. 1a).
2. Inhomogeneous shell–like distribution of the circumstellar dust caused by the variation of temperature, density, and chemical composition in the dust forming region (Fig. 1b, 1c).
3. Substantial backwarming of the atmosphere inside the dust forming region due to the dust opacity, where in turn the temperature increase terminates the condensation process (Fig. 1d).

Fleischer et al. (1995) showed, that the dust formation process in the circumstellar shell is controlled by a timescale of its own, which differs from the timescale of the interior pulsation. This timescale is decisively controlled by the carbon abundance. Depending on its value, the spatial structure of the models repeats after one pulsation period, or after multiples of the period (*Multiperiodicity*), or it even does not repeat at all. In the latter case dust formation still takes place in regular intervals, but the local conditions and thus the condensation efficiency are different, resulting in an irregular pattern, as in the model presented here.

The spatial structure of the dust shell models and its time variation manifests itself in the optical appearance. The calculated brightness profiles show a step–like structure on a scale of a few stellar radii, corresponding to the discrete shell–like distribution of the dust (Winters et al. 1995). The synthetic infrared lightcurves follow the periodic variation of the luminosity with superimposed shifts of the mean magnitude and changes of the amplitude, which reflect the long–term variations of the spatial structure of the outflow (Winters et al. 1994). Similar behavior has been reported for observed lightcurves of actual objects (Le Bertre 1992).

4 Infrared CO line profiles from variable dust shells

4.1 Molecular line calculations

Based on the radial structures for the velocity, the density and temperature, which result from the dynamical model calculations, the synthetic CO infrared line profiles for the fundamental $(1-0)$ and first overtone $(2-0)$ transitions are calculated employing a three–step procedure (see Keady 1982 and Keady et al. 1988 for more details).

At first the underlying infrared continuum is determined from the solution of the static transfer equation in spherical symmetry assuming radiative equilibrium according to the method of Leung (1975, 1976).

Then, the line radiative transfer is calculated according to the comoving frame method of Mihalas et al. (1975). To solve the coupled radiative transfer and statistical equilibrium equations we apply the equivalent two–level atom formalism (see Mihalas et al. 1975), assuming complete redistribution and rotational LTE, but allowing for vibrational non–LTE. Because previous non–LTE calculations indicated that the CO vibrational level populations are essentially in equilibrium with the dust temperature in optically thick dust shells, the vibrational level populations are determined from a Boltzmann distribution at the dust temperature in the present calculations.

Once the comoving frame source functions of the spectral lines are determined, the formal solution of the observer's frame radiation transport equation is integrated along characteristic rays to obtain the emergent intensity, from which the flux profiles are calculated. The presence of a highly nonmonotonic velocity field necessitates several grid refinements to ensure that all of the intensity is properly sampled.

Finally all calculated line profiles have been Fourier smoothed to the instrumental resolution for easy comparison with the observations.

The observations of the CO fundamental and overtone lines were obtained at the KPNO Mayall 4 meter telescope using the Fourier Transform spectrometer at the coude focus. The typical integration times are 2 – 3 hours for the $5\mu m$ fundamental lines and up to 10 hours for the $2\mu m$ overtone lines. The resolution varies from $2-4$ kms^{-1}, and the ratios of peak signal to rms noise are typically in excess of several hundred to one.

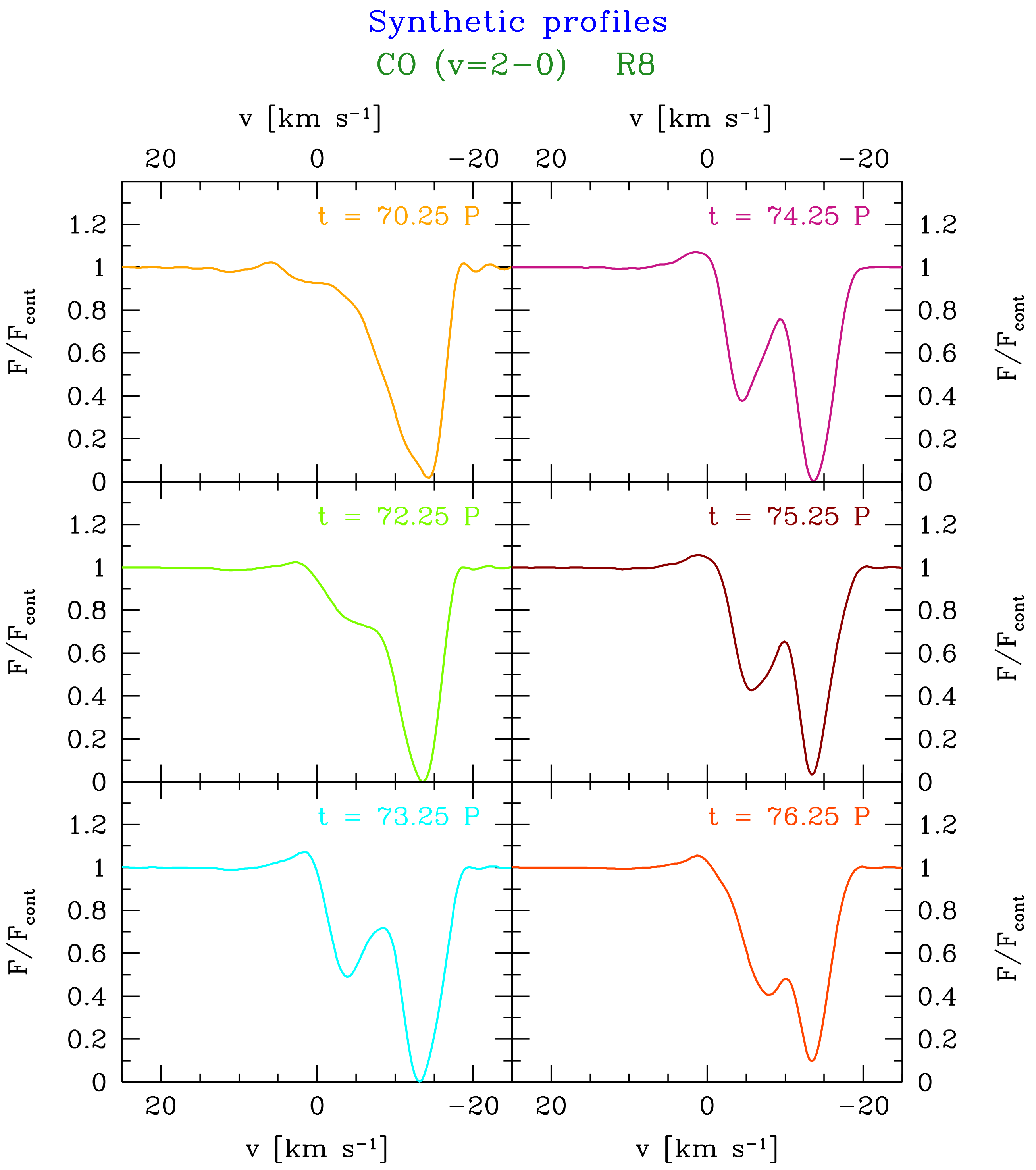

Figure 3: Synthetic CO ($v = 2 - 0$) first overtone line profiles at different instants of time. Between $t = 70.25$P and $t = 73.25$P a strong absorption feature evolves around 5 km s^{-1}.

4.2 Synthetic line profiles and comparison with observations

Figure 3 shows the synthetic line profiles of the CO $v = 2-0$ R8 overtone line at different instants of time. As in the observed spectra (Fig. 1) the absorption extends from about zero velocity to ≈ -17 kms^{-1}, and the main absorption core is located at ≈ -14 kms^{-1}, showing slight variations of its strength and exact location with time. After $t = 70.25$ P a secondary absorption feature starts to develop at ≈ -5 kms^{-1}, which considerably increases its strength during the following time interval, and simultaneously shifts to higher velocities.

> **The emergence and the temporal evolution of the secondary absorption feature can be interpreted to be the result of the formation of a new dust layer.**

The radial structure of the dust shell model was shown in Fig. 2 at $t = 72.25$ P and $t = 73.25$ P, i.e. at two phases enclosing the development of the feature. During this time a new dust layer is formed around $5\,R_0$, as indicated by the degree of condensation. The radiation pressure acting on this dust leads to the acceleration of a dust amplified shock starting at a material velocity < 5 kms^{-1}, and to an enhanced density of the matter overrun by the shock in the region around $5\,R_0$. Subsequently the velocity of the accelerated material increases further, while its temperature and density at the corresponding positions decrease due to the expansion. Thus, the secondary absorption feature at first gets stronger until it weakens again after $t = 74.25$ P, simultaneously moving from -5 kms^{-1} to higher velocities.

In Fig. 4 the temporal evolution of the synthetic line profiles is compared with observed $2-0$ overtone lines from IRC+10216. The dates of the observations are separated by ≈ 2.5 P and ≈ 3.5 P, where $P = 650$ d is the pulsation period adopted for IRC+10216. The observed spectra nicely show the development of a low–velocity absorption around -5 kms^{-1}, and it is worth noting that this feature evolves on approximately equal timescales in the observations and the calculations. However the calculated lines are too strong indicating that the CO density and, thus, pssibly the mass loss rate in the model, is too high by about a factor of three.

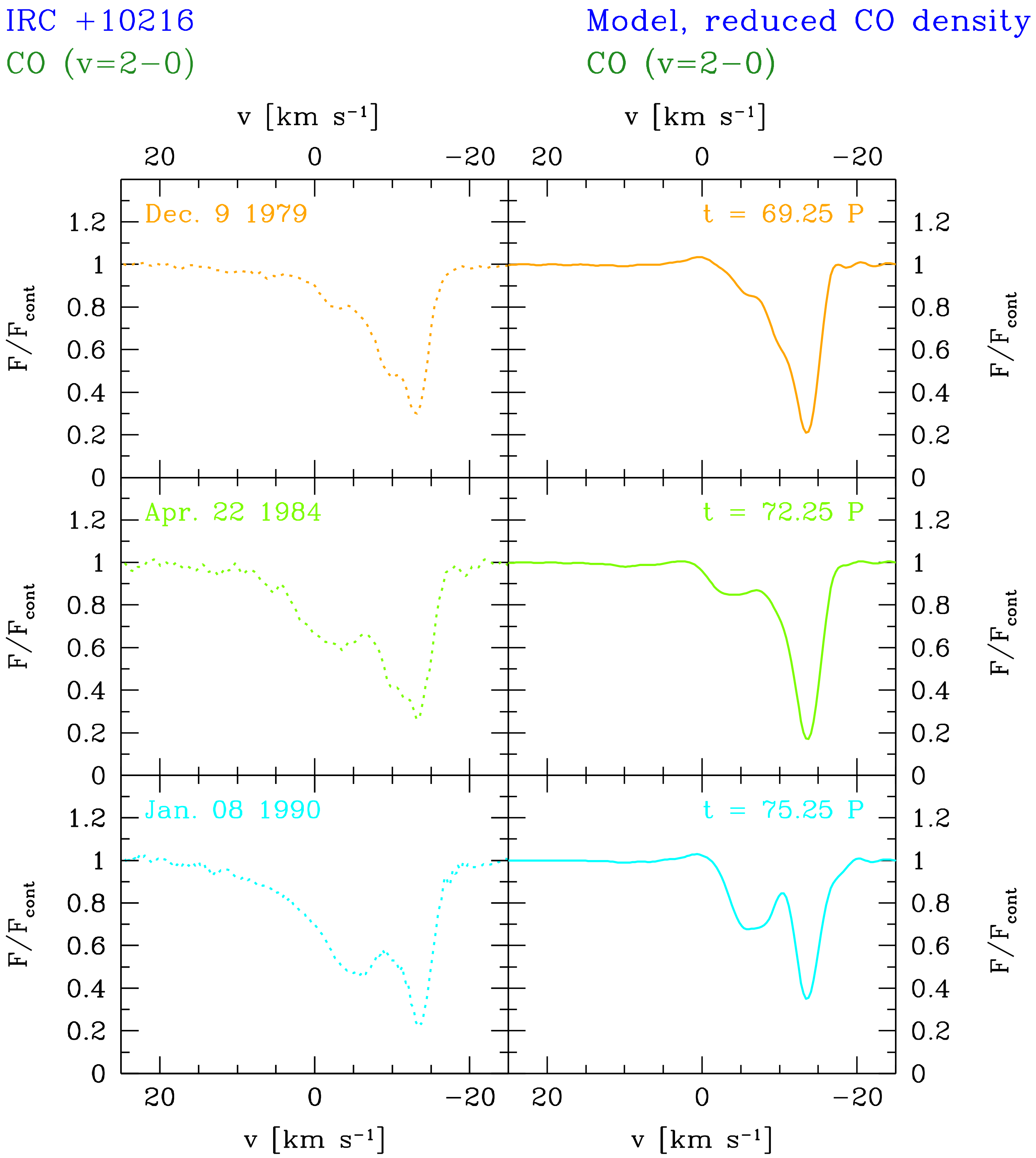

Figure 4: Temporal variation of low excitation CO first overtone line profiles.
left column: Observed line profiles from IRC+10216 (Sada 1993).
right column: Calculated line profiles. The CO abundance has been reduced by a factor of 0.33 in order to match the observed line strengths.
Note that the low–velocity absorption feature evolves on approximately equal timescales in the observations and the calculations

5 Conclusions

Our dynamical dust shell models, which result from a consistent treatment of time–dependent hydro– and thermodynamics, (continuum) radiative transfer, chemistry and carbon grain formation, clearly demonstrate that both, the pulsation of the central star and the condensation of grains in the circumstellar shell, are key processes controling the structure and the temporal evolution of the winds from long–period variables. Their complex non–linear interaction gives rise to a number of dust induced phenomena, which affect the observed properties of such winds, e.g. the spatial brightness distribution or the infrared lightcurves.

The synthetic CO infrared line profiles calculated on the basis of a dynamical dust shell model for IRC+10216 resemble the multicomponent structure and the time variations of corresponding lines in the observed spectra, which thereby are explained as a consequence of the dynamical structure and its temporal variation in the inner parts of the wind. Especially the emergence and subsequent evolution of a secondary low–velocity absorption feature in the first overtone lines can be understood as a result of the formation of a new dust layer and the subsequent acceleration of the matter by radiation pressure on dust. However, the line strengths of the calculated first overtone lines are too high, indicating that the CO density and, thus, possibly the mass loss rate of the dust shell model is too large and should be closer to a value of $\approx 1\ 10^{-5}\ \mathrm{M}_\odot\,\mathrm{yr}^{-1}$.

Nevertheless, the qualitative agreement of several derived observable properties (lightcurves, brightness distributions, CO line spectra) with respective observations gives us confidence, that our dust shell models reproduce the characteristic properties of the spatial structure and the time variability of cool dusty winds from Miras and long–period variables.

Acknowledgements

This work has been partly supported by the BMBF (grant 05 3BT13A 6) and the DFG (Se 420/5–4). Research at Los Alamos National Laboratory was performed under the auspices of the U.S. Department of Energy.

References

Bowen G.H., 1988, ApJ 329, 299

Fleischer A.J., Gauger A., Sedlmayr E., 1991, A&A 242, L1

Fleischer A.J., Gauger A., Sedlmayr E., 1992, A&A 266, 321

Fleischer A.J., Gauger A., Sedlmayr E., 1995, A&A 297, 543

Gail H.-P., Sedlmayr E., 1988, A&A 206, 153

Gauger A., Gail H.-P., Sedlmayr E., 1990, A&A 235, 345

Habing H.J., 1990, in: From Miras to Planetary Nebulae: Which Path for Stellar Evolution?, M.O. Mennessier and A. Omont (eds.), Editions Frontières, Gif sur Yvette, p.16

Hashimoto O., 1995, ApJ 442, 286

Hinkle K.H., Scharlach W.W.G., Hall D.N.B., 1984, ApJS 56, 1

Keady J.J., 1982, The circumstellar envelope of IRC+10216, PhD thesis, New Mexico State University, Las Cruces

Keady J.J., Hall D.N.B., Ridgway S.T., 1988, ApJ 326, 832

Knapp, G.R., 1987 in: Late Stages of Stellar Evolution, S. Kwok and S.R. Pottasch (eds.), Reidel, Dordrecht, p. 103

Le Bertre, T., 1992, A&AS 94, 377

Leung C.M., 1975, ApJ 199, 340

Leung C.M., 1976, JQSRT 16, 559

Lucy L.B., 1976, ApJ 205, 482

Mihalas D., Kunasz P.B., Hummer D.G, 1975, ApJ 202, 465

Richtmyer R.D., Morton K.W., 1967, Difference methods for initial–value problems, 2nd ed., John Wiley & Sons, New York

Sada P.A.V., 1993, Temporal variations in the circumstellar shell of IRC +10216, PhD thesis, New Mexico State University, Las Cruces

Winters J.M., Fleischer A.J., Gauger A., Sedlmayr E., 1994, A&A 290, 623

Winters J.M., Fleischer A.J., Gauger A., Sedlmayr E., 1994, A&A 302, 483